ChemPubSoc Europe

DOI: 10.1002/chem.201502211

CHEMISTRY A European Journal Full Paper

Drug Design | *Very Important Paper* |

VIP Activation of Hsp90 Enzymatic Activity and Conformational Dynamics through Rationally Designed Allosteric Ligands

Sara Sattin,[a] Jiahui Tao,[b] Gerolamo Vettoretti,[c] Elisabetta Moroni,[c] Marzia Pennati,[d] Alessia Lopergolo,[d] Laura Morelli,[a] Antonella Bugatti,[e] Abbey Zuehlke,[f] Mike Moses,[f] Thomas Prince,[f] Toshiki Kijima,[f] Kristin Beebe,[f] Marco Rusnati,[e] Len Neckers,[f] Nadia Zaffaroni,[d] David A. Agard,[b] Anna Bernardi,[a] and Giorgio Colombo*[c]

Abstract: Hsp90 is a molecular chaperone of pivotal importance for multiple cell pathways. ATP-regulated internal dynamics are critical for its function and current pharmacological approaches block the chaperone with ATP-competitive inhibitors. Herein, a general approach to perturb Hsp90 through design of new allosteric ligands aimed at modulating its functional dynamics is proposed. Based on the characterization of a first set of 2-phenylbenzofurans showing stimulatory effects on Hsp90 ATPase and conformational dynamics, new ligands were developed that *activate* Hsp90 by targeting an allosteric site, located 65 Å from the active site. Specifically, analysis of protein responses to first-generation activators was exploited to guide the design of novel derivatives with improved ability to stimulate ATP hydrolysis. The molecules' effects on Hsp90 enzymatic, conformational, co-chaperone and client-binding properties were characterized through biochemical, biophysical and cellular approaches. These designed probes act as allosteric activators of the chaperone and affect the viability of cancer cell lines for which proper functioning of Hsp90 is necessary.

Introduction

The dynamic properties of proteins are critical for the functions they exhibit.[1] They can be finely tuned through allostery, a general property of biomolecules whereby a perturbation at one site leads to a response at another, turning specific functional states on or off.[2] Allosteric ligand binding provides the opportunity to regulate protein functions with small molecules that act at a distance from the active site, without directly interfering with its chemical activity.[1,3] Additionally, allosteric ligands can be used to modulate the equilibrium and dynamics of distinctive protein states implicated in certain cellular pathways and phenotypes.[4]

The fundamental chemical challenge for the discovery of allosteric protein modulators consists in identifying privileged structures that selectively target key protein substates involved in the regulation of biochemical function. To progress along this appealing avenue, we focused on the 90 kDa heat shock protein (Hsp90) molecular chaperone. This protein is known to undergo a complex dynamic cycle, which is essential to its chaperone activity that, in turn, regulates the state of a number of client proteins in the cell. Hsp90 integrates different pathways required for cell development and maintenance.[5] and plays a key role in the regulation of a wide variety of so-called client proteins.[6] As such, it has been proposed as an interesting target in cancer,[7] vascular disease,[8] neurodegeneration,[9] and as a major player in evolution.[10] Thanks to its dynamic nature[5,11] Hsp90 influences the functional lifetime of many clients that vary widely in sequence, structure, size and function.[12] In eukaryotes this activity is further regulated by a number of co-chaperones, which bind individual Hsp90 states populated at different stages of the chaperone cycle. Hsp90 dynamics depend on ATP binding and hydrolysis, which underlie the onset of conformational transitions between substates with different functional properties.[13] Here, we set out to develop a rational approach to regulate the ATPase activity

[a] *Dr. S. Sattin,[+] Dr. L. Morelli, Prof. A. Bernardi*
Dipartimento di Chimica, Università degli Studi di Milano
via Golgi, 19, 20133, Milan (Italy)

[b] *Dr. J. Tao,[+] Prof. D. A. Agard*
Howard Hughes Medical Institute and Department of Biochemistry and Biophysics, University of California
600 16th Street, San Francisco, 94158 (USA)

[c] *Dr. G. Vettoretti,[+] Dr. E. Moroni,[+] Dr. G. Colombo*
Istituto di Chimica del Riconoscimento Molecolare, CNR
via Mario Bianco, 9, 20131, Milan (Italy)
E-mail: giorgio.colombo@icrm.cnr.it

[d] *Dr. M. Pennati, Dr. A. Lopergolo, Dr. N. Zaffaroni*
Dept. Experimental Oncology and Molecular Medicine
Molecular Pharmacology Unit
Fondazione IRCCS Istituto Nazionale dei Tumori
via Amadeo, 42, 20133 Milano (Italy)

[e] *Dr. A. Bugatti, Dr. M. Rusnati*
Department of Molecular and Translational Medicine
University of Brescia, Viale Europa 11, 25123, Brescia (Italy)

[f] *Dr. A. Zuehlke, Dr. M. Moses, Dr. T. Prince, Dr. T. Kijima, Dr. K. Beebe, Dr. L. Neckers*
Urologic Oncology Branch, Center for Cancer Research
National Cancer Institute, 9000 Rockville Pike, Bethesda, MD 20892 (USA)

[+] *These authors contributed equally to this work.*

Supporting information for this article is available on the WWW under http://dx.doi.org/10.1002/chem.201502211.

© 2015 Wiley-VCH Verlag GmbH & Co. KGaA, Weinheim

and conformational dynamics of Hsp90 through designed allosteric small molecule ligands.

Hsp90 functions as a homodimer (Figure 1). Crystal structures from different organisms highlighted a common modular organization in terms of N-terminal (NTD), middle (M) and C-terminal (CTD) domains.[14] The CTD is the dimerization domain, while the NTD contains an ATP-binding site. ATPase activity requires transient dimerization of the NTD in a closed state of the dimer and is essential for the Hsp90 working cycle. The exact mechanism of coupling between ATP-binding/hydrolysis and client folding remains elusive. Yet, structural and biochemical data support a model in which nucleotide binding at the NTD propagates a conformational signal to the CTD,[14d] while the chaperone undergoes conformational rearrangements that bring the two NTDs into close association in the ATP-state, but not in the ADP or apo states. Formation of the closed state can be induced by ATP or the non-hydrolyzable analogue adenosine 5′-(β,γ-imido)triphosphate (AMP-PNP). Upon ATP hydrolysis, the protein cycles back to the open, ADP-bound state. A number of intermediate conformational states have also been characterized, that are induced or stabilized by interaction with different clients or co-chaperone proteins.[13,15] Figure 1 highlights some of these interactions, with the co-chaperones Aha1, an endogenous activator of Hsp90 ATPase activity, and Sba1, an Hsp90 inhibitor, which acts by binding to the closed conformation and blocking the chaperone dynamics. The predicted allosteric site that we sought to exploit (AS, Figure 1)[16] is located at the MD/CTD interface, a region where the model client Δ131Δ is also known to interact.

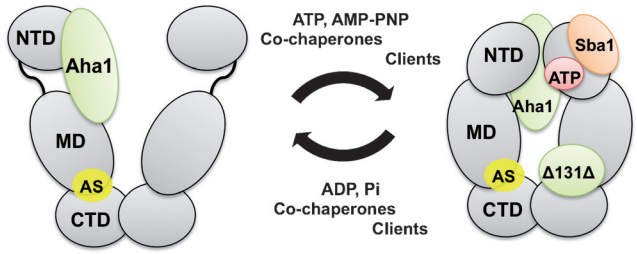

Figure 1. Schematic representation of Hsp90 structure and its conformational equilibrium. NTD, N-terminal domain; MD, middle domain; CTD, C-terminal domain; AS, predicted allosteric site; Aha1, Hsp90 co-chaperone; Sba1, yeast homologue of co-chaperone p23; Δ131Δ, Hsp90 client protein model.

Most known small molecule Hsp90 modulators interact with the protein at the NTD and inhibit Hsp90 ATPase activity.[17] They include radicicol and geldanamycin or its derivative, 17AAG.[18] Some of such inhibitors have entered clinical trials as antitumor drugs but have shown severe limitations. Indeed, blocking the ATPase activity of Hsp90 induces the so-called heat shock response, a prosurvival mechanism mediated by HSF-1 (heat shock factor 1), which limits the action of the drug.[19]

Rationally designed chemical probes can be used to select and activate, and not only to inhibit, Hsp90 key substates, providing a connection between protein activities and possible cellular outcomes. Here, we pursue the first *rational* design of chemical activators of Hsp90 functions aimed to target sites alternative to the ATP site, and investigate their effects on the chaperone conformational dynamics, enzymatic, binding and cellular properties.

In this study, we build on the results of recently developed computational methods that unveiled the presence of a druggable site in Hsp90 CTD[16,20] and facilitated the design of small molecules able to bind it.[21] Different sets of experiments showed that the *O*-aryl rhamnoside (**1**; Figure 2 A) identified through this method could bind the C-terminal domain of Hsp90 and exert interesting antitumor activities.[16] Here, we evolve **1** into new chemical entities that enable controlled activation of Hsp90 ATPase function. We show that designed derivatives are genuine allosteric ligands with a structure-dependent ability to stimulate Hsp90 ATPase and to alter conformational dynamics favoring synergistic effects with the activating co-chaperone Aha1, to modulate Hsp90 direct interactions with the co-chaperone Sba1 (p23), and to compete with the model client protein Δ131Δ. We characterize the impact of small molecule induced activation on Hsp90 interactions in vitro and on the stability of a number of clients in cellular models, and we investigate the possibility that acceleration of conformational dynamics may in fact represent a new way of perturbing the chaperoning mechanisms that underlie cell viability; indeed, some of our compounds inhibit the proliferative potential of tumor cells including those resistant to Hsp90 ATP-competitive inhibitors.

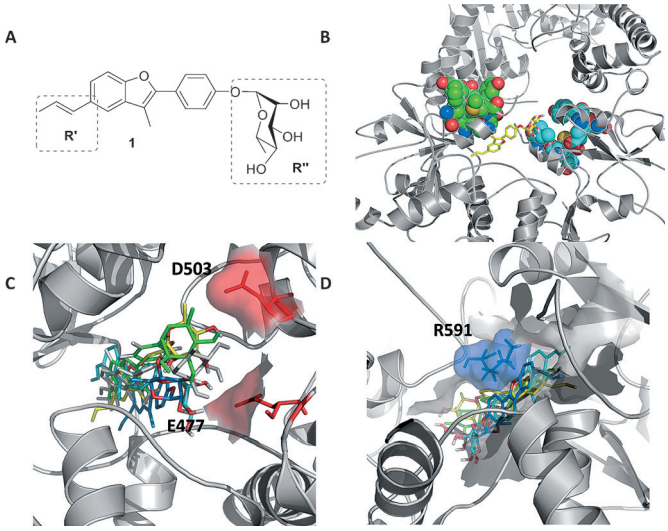

Figure 2. Structure of the initial lead and interaction with Hsp90 allosteric site. A) Molecular structure of **1**; B) 3D structure of compound **1** (yellow) in complex with the closed structure of Hsp90. The van der Waals spheres in light blue and green indicate the client protein Δ131Δ binding site. C) Representative poses of **1** in the representative conformations of the allosteric site, showing the contacts of the ligand with E477 and D503 on protomer A. D) Contacts of **1** with protomer B, highlighting interaction with R591.

© 2015 Wiley-VCH Verlag GmbH & Co. KGaA, Weinheim

Results and Discussion

Design and synthesis of first-generation Hsp90 modulators

In our previous work, the rhamnoside **1** (Figure 2A) was selected from the NCI library by virtual screening in a 3D pharmacophore designed to complement the stereoelectronic properties displayed by an allosteric site in the CTD. The site was identified through the analysis of long-range dynamic communication mechanisms with the ATP-site, using the coordination propensity (CP) parameter (see the Supporting Information).[16,20] It comprises residues at the CTD interface with the M-domain, which define a druggable pocket coincident with the region of a recently identified binding site for the model client protein $\Delta131\Delta$[22] (Figure 2B). The long-range coordination properties of the amino acids defining the allosteric pocket describe their dynamic connection to events occurring in the orthosteric ATP binding site, and are conserved across different members of the Hsp90 family.[20a] Targeting these residues by designed ligands, such as **1**, should thus provide a way of influencing the functional properties of the protein.[23] Indeed, **1** was found to bind the Hsp90 C-terminal domain disrupting chaperoning functions and to exhibit antiproliferative activity in different tumor cell lines.[23]

To optimize the structure and functional impacts of this lead, in the absence of crystal structures, we investigated binding determinants in the allosteric site through docking calculations. It should be noted here that no X-ray structure of any C-terminal ligands in complex with Hsp90 has been determined so far. The initial target was the MD-relaxed ATP-bound Hsp90 structure used for the pharmacophore-based discovery of **1**.[16,23] Considering the flexibility of the protein and of the allosteric pocket,[21a] we selected an ensemble approach to characterize chaperone–ligand interactions. The minimum energy pose of the **1**–Hsp90 complex (Figure 2B) was used as input for long timescale MD simulations, including ATP at the NTD. The aim was to identify the hot spots of the allosteric site where key functional groups on the ligand best complement the receptor, taking the dynamic exchange between the binding partners explicitly into account.

Structural cluster analysis of the resulting trajectory (see the Supporting Information) showed that the first ten clusters recapitulated approximately 95% of the protein structural variability. The RMSD between visited pocket conformations in the putative binding site (Table S1 in the Supporting Information) reached to 4 Å, revealing the diversity induced by **1**. Such differences, due to the cross-talk between the protein and the ligand, were not expected a priori and revealed protein conformations that could play a role in small molecule recognition. The resulting structures were next used to explore possible alternative poses of **1** in the allosteric site. The compound was redocked into each of the ten representative structures. The resulting structural ensembles were used to generate a consensus model of Hsp90 residues and functional groups on **1** that define the most relevant stabilizing contacts (Figure 2C and D). Two areas where functional group diversification on the lead could translate into a modulated response of the chaperone were identified: the carbohydrate moiety (R″, Figure 2A), which in the consensus model points towards an area lined by E477 and D503 (Figure 2C), and the propenyl group (R′, Figure 2A), which contacts a hydrophobic pocket also lined by R591 from the other protomer (Figure 2D).

To validate this model and to expand the available SAR, glycodiversification of the 2-phenylbenzofuran aglycone **2** (Table 1) was examined. Glycorandomization is a well-known strategy to tune the activity of a variety of glycoconjugates against their protein targets[24] and is an attractive avenue for the case at hand, where computational data indicate a strong involvement of the sugar moiety in the interaction with Hsp90 allosteric site. A first series of molecules **4** to **16** was synthesized (Table 1) by glycosylation of **2** and of the 5-chloro analogue **3** (an intermediate in the synthesis of **2**), as previously reported in ref. [25]. The full structures of all compounds are reported in Figure S1 in the Supporting Information.

Table 1. First generation of CTD ligands **1**–**16**.[a]

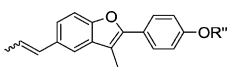

2 R″ = H

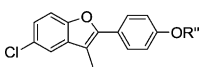

3 R″ = H

R″		R″	
1	α-L-Rha	4	α-L-Rha
5	β-D-Glc	6	β-D-Glc
7	β-L-Glc	8	β-L-Glc
9	α-D-Man	10	α-D-Man
11	β-D-Gal	12	β-D-Gal
13	β-L-Gal	14	β-L-Gal
15	β-L-Fuc	16	β-L-Fuc

[a] The propenyl scaffold **2** was used as an *E/Z* mixture after checking that the natural compound **1** and *E/Z*-**1** had a comparable effect on the protein activity.

Designed allosteric ligands stimulate Hsp90 ATPase activity

To characterize their role as allosteric modulators, we measured the effects of compounds **1**–**16** on the ATPase activity of the Hsp90 yeast homologue (Hsc82).[26] Interestingly, most compounds, including **1**, turned out to be *activators* of ATP hydrolysis (Figure 3, compounds **1** and **4**–**16**), with variable potency, depending on the type of carbohydrate moiety and benzene ring substitution (propenyl or chlorine). Compounds **4** and **10**–**12** were the strongest activators of Hsp90 with a two- to threefold enhancement of ATPase rate. Since the basal ATPase rate of yeast Hsp90 is very low, this kind of acceleration is not negligible, it has very little precedent in the literature, and *none with rationally designed compounds*.[27]

From a ligand-design point of view, the data indicate that a chlorine atom in position R′ (Figure 2) is as good as, and often better than, the original propenyl substitution (compare pairs **1** and **4**, **9** and **10**, **11** and **12**). Additionally, a significant effect of the sugar on the level of activity was observed, with D-mannose (as in **10**) and D-galactose (as in **12**) emerging as privileged fragments alongside L-rhamnose (in **4**).

© 2015 Wiley-VCH Verlag GmbH & Co. KGaA, Weinheim

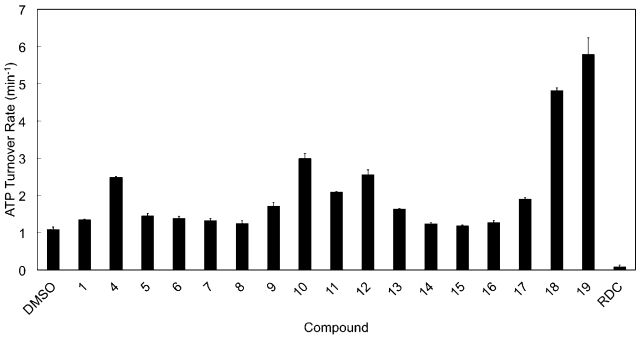

Figure 3. Effects of benzofurans **1**–**19** in stimulating yeast Hsp90 (Hsc82) ATPase activity. ATP hydrolysis rate of Hsp90 was measured in the presence of the compounds (50 μM) or radicicol (RDC, 5 μM). The ATP turnover rate is reported as the mean of four independent measurements. Basal Hsc82 ATPase activity was measured using DMSO alone.

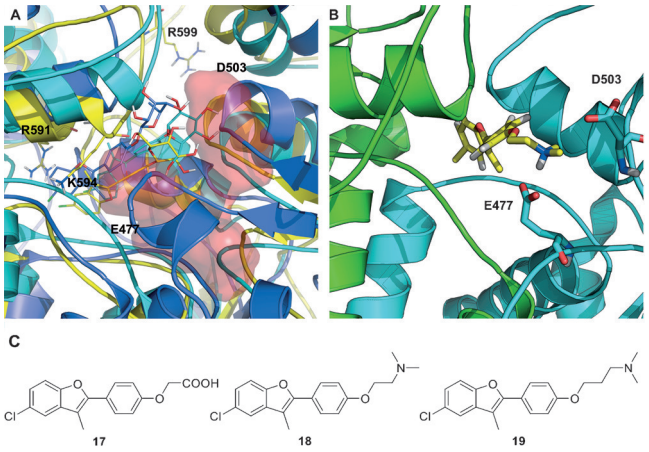

Figure 4. Model structures of first-generation allosteric ligands in an ensemble of conformations of the putative allosteric pocket. A) Representative structures of the poses of compounds **4** (blue), **10** (cyan) and **12** (yellow). The red surfaces indicate the locations of charged residues targeted by the ligands. B) Representative structure of compound **18** in the allosteric binding pocket. The two Hsp90 protomers are colored differently. C) Compounds **17** to **19**.

Rational optimization of first-generation ligands further increases Hsp90 ATPase activity

Starting from the aforementioned observations, to design improved allosteric activators we docked all the first-generation compounds into the ten Hsp90 conformations used for the first generation of derivatives, describing binding in terms of an ensemble of ligand poses in complex with an ensemble of protein structures.[28]

All glycosylated compounds explored common ensembles in the allosteric site, similar to **1**. Representative poses are shown in Figure 4A for compounds **4** (blue) **10** (cyan) and **12** (yellow; Figure 4A). The pair formed by the negatively charged E477 and D503 on one protomer, towards which initial design was aimed, was always engaged in hydrogen bonding interactions with the carbohydrate moieties (R″). The most active glycosylated compounds, **10** and **12**, showed two hydroxyl groups (on C-6 and C-4 of the sugar) ideally oriented to establish H-bonding interactions with the aforementioned negative residues. This interaction was reinforced by a H-bond network involving R591, R599 and the hydroxyl groups on the carbohydrate ring. On the R′ side, two positively charged residues from the other protomer, R591 and K594, were involved in stabilizing interactions with the halogen of compounds deriving from the common intermediate **3**.

On this basis, a second group of ligands (**17**–**19**) was designed to exploit potential productive interactions with the network of charged amino acids (Figure 4B and C) in the allosteric pocket. Indeed, **18** and **19** were found to dramatically accelerate yeast Hsp90 (Hsc82) ATPase rate (by up to sixfold, Figure 3), providing further support to our model and to the design approach. Absolute k_{cat} values are reported in Table S2 in the Supporting Information.

The ability of the best stimulating compounds to effectively bind the Hsp90-CTD was proven by preliminary surface plasmon resonance experiments (SPR; Table S3 in the Supporting Information); all compounds bound Hsp90-CTD in a dose-dependent manner (data not shown). There is no correlation between the observed effects on ATPase acceleration and the estimated binding affinity values. However, this result could actually be expected for allosteric modulators. A full understanding of the structure–activity relationship for these molecules will require an atomic level analysis of the molecular mechanisms leading to the observed acceleration effects. These studies are currently in progress in our laboratories and some emerging elements are described in the following section.

Allosteric ligands accelerate Hsp90 conformational dynamics

The conformational change of Hsp90 initiated by ATP and non-hydrolyzable ATP analogues is a hallmark of the Hsp90 cycle.[29] ATP and non-hydrolyzable ATP analogues such as AMP-PNP induce a closed state of the Hsp90 dimer, where the NTD of the two protomers are in close proximity (Figure 1). As previously mentioned, this is the catalytically active state of the protein that allows ATPase activity. We measured the closure rate in the presence of the allosteric modulators by FRET, using an Hsp90 dimer with one protomer labeled with a FRET donor (Alexa Fluor 555) and the other with a FRET acceptor (Alexa Fluor 647). The addition of AMP-PNP drives the closure of Hsp90, which shortens the distance between the FRET dyes, resulting in an increased FRET signal (DMSO, Figure 5). Similar to the ATPase results, **10**, **12**, **18** and **19** most accelerated the Hsp90 conformational change process, consistent with the observation that N-domain closure is the rate-limiting step for ATP hydrolysis. The NTD inhibitor radicicol was used as negative control (RDC, Figure 5) and, as expected, it did not influence the closure rate of the protein to any measurable extent, preventing N-terminal dimerization. The FRET traces for all compounds are reported in Figure S2 in the Supporting Information. The rate constants of the closing kinetics in the presence of the designed compounds are reported in Table S4 in the Supporting Information.

© 2015 Wiley-VCH Verlag GmbH & Co. KGaA, Weinheim

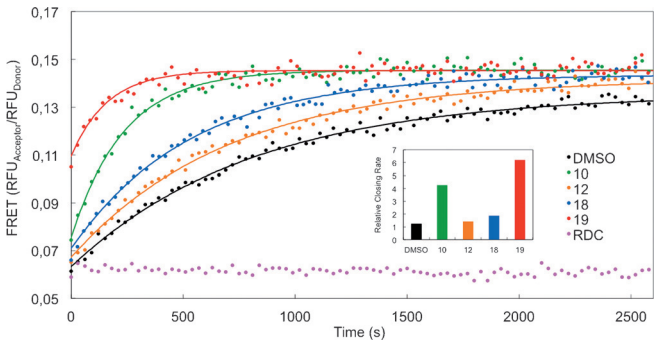

Figure 5. FRET-based measurement of yeast Hsp90 (Hsc82) conformational change. Hsp90 conformational change rate measured by the FRET-based assay in the presence of allosteric activators, compared to the NTD inhibitor radicicol (RDC). Conformational dynamics were initiated by adding AMP-PNP (1 mM) in the presence of 50 μM test compounds. The rates in the inset are calculated by exponential fitting of the data relative to control DMSO/AMP-PNP.

The 2-phenylbenzofuran derivatives thus have an actual impact on modulating both the mechanisms of formation and the conformational properties of the catalytic state of Hsp90.

Since compounds **10**, **12**, **18** and **19** stood out as giving a significant acceleration of the chaperone enzymatic activity, their effects were also tested on human Hsp90α. In this case, only compounds **18** and **19** proved able to significantly stimulate ATPase. It is worth considering here that the activity of human Hsp90 is about an order of magnitude lower than that of the yeast chaperone, which may explain the observation of stimulation only for the most active compounds (Figure S3 in the Supporting Information).

Overall the results of our design efforts, based on the computational mapping of the stereochemical and dynamic properties of the identified allosteric site, are consistent with a model in which the compounds bind to the boundary between the M- and C-terminal domains and modulate both Hsp90 enzymatic properties and its ability to form the N-terminal dimerization state, resulting in accelerated ATPase activities, in line with the general mechanism reported in.[30]

Designed allosteric activators synergize with Aha1 to accelerate Hsp90 ATPase cycle

The most relevant known natural activator of the Hsp90 ATPase cycle is the co-chaperone protein Aha1, an endogenous accelerator.[31] Aha1 is known to bind Hsp90 engaging the N- and middle domains of the chaperone in its open conformation (Figure 1) and to accelerate ATPase by an order of magnitude.[31] The ATPase acceleration observed with the designed benzofurans prompted the question whether they are in competition or synergistic with the action of Aha1: allosteric compounds designed to target the MD/CTD interface should arguably not compete with the co-chaperone binding or inhibit its activity. The effects of allosteric derivatives on yeast Hsp90 (Hsc82) were then measured in the presence of yeast Aha1. The compounds did not abolish the acceleration of Hsp90 ATPase by Aha1, but rather amplified the co-chaperone effects in a synergistic fashion (Figure 6). In all cases examined the ATP hydrolysis rates were one order of magnitude higher that those measured without Aha1 (Figure 3), but the relative trend of the values was once again determined by the nature of the modulators.

The results described above suggest that the regulation of ATPase activity by the designed benzofurans occurs through an alteration of the overall protein dynamics, controlled by the allosteric site. This interpretation was supported by data obtained from co-immuno precipitation (Co-IP) experiments performed in protein lysates of yeast expressing His-tagged Hsc82. In the presence of ATPase stimulatory compounds endogenous Aha1 association with Hsc82 was generally increased while the nucleotide-dependent dissociation of the complex was inhibited (Figure 7A).

In this context, we also examined whether the compounds altered the interaction between Hsc82 and the co-chaperone

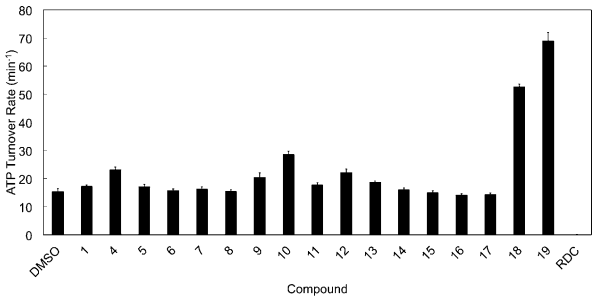

Figure 6. Synergistic stimulation of yeast Hsp90 (Hsc82) ATPase by Aha1 and compounds **1**–**19**. ATP hydrolysis rate of Hsc82 was measured in a similar manner as in Figure 3, but in the presence of yeast Aha1 (2 μM). The ATP turnover rate is reported as the mean of four independent measurements.

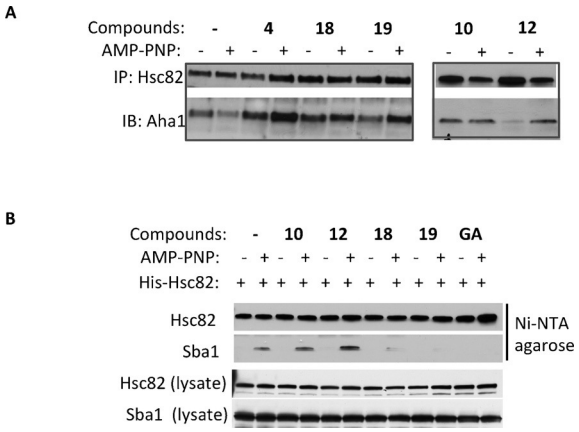

Figure 7. Effects of allosteric ligands on yeast Hsp90 (Hsc82) interaction with co-chaperones. A) Interactions with the ATPase stimulatory co-chaperone Aha1. Results of co-immuno precipitation (Co-IP) experiments show that **4**, **10**, **12**, **18** and **19** all potentiate yeast Aha1 interaction with yeast Hsp90 while also minimizing the ability of nucleotide to promote dissociation of Aha1. B) Interactions with the ATPase inhibitory co-chaperone Sba1. The presence of allosteric accelerators minimizes AMP-PNP-dependent association of Sba1 (p23) with Hsc82. These data were obtained by adding compounds to yeast lysates followed by affinity pulldown of His-tagged Hsc82 with Ni-NTA agarose beads. Hsc82 and Sba1 were visualized in pulldowns and lysate with appropriate antibodies (see the Experimental Section).

© 2015 Wiley-VCH Verlag GmbH & Co. KGaA, Weinheim

Sba1 (yeast p23, Figure 1). Sba1 is an inhibitor of ATP hydrolysis that operates by interacting with the N-dimerized, "closed" Hsp90 conformation poised for hydrolysis (Figure 1), stabilizing it and thus blocking the chaperone dynamic cycle.[15a] AMP-PNP was added to the lysates to induce N-dimerization of the chaperone. After selective isolation of His-tagged Hsc82 using Ni-NTA agarose resin, Western blotting was performed to visualize associated Sba1. In line with the kinetic data presented above (Figure 5), the most potent allosteric stimulators (compounds **18** and **19**) abrogated AMP-PNP-dependent Sba1/Hsc82 interaction (Figure 7B), suggesting that they can either alter the closed state recognized by Sba1 or simply accelerate the chaperone cycle, reducing its population. For comparison, the last two lanes of the blot show that the ATP competitive Hsp90 inhibitor geldanamycin (GA), which prevents N-domain dimerization, also abrogates Sba1 interaction with Hsc82 (Figure 7B).

Combining these observations with the FRET data (Figure 5), we suggest that the allosteric modulators modify the kinetics between Hsp90 open and closed forms, which reverberates in an altered population of the structural ensemble presented to co-chaperones, favoring Aha1 recruitment and disfavoring Sba1 binding. Additionally, it can be argued that the allosteric ligands could alter the geometric properties of the closed state, modulating co-chaperone affinities. However, in the absence of X-ray based experimental structures of the complexes, this point represents a possible working hypothesis.

In summary, our data support a model in which not only designed compounds do show a significant acceleration of Hsp90 ATPase, but also a consistent synergistic stimulation with Aha1, suggesting that the compounds and the co-chaperone do not compete with one another for binding Hsp90, while modifying the same rate-limiting conformational process by distinct but complementary interactions. The data also confirm that ATPase stimulation is likely due to an acceleration of the chaperone conformational cycle, and as such are similar to other recent findings demonstrating that enforced N-domain proximity (without N-domain dimerization) is sufficient to enhance Hsp90 ATPase activity while retaining further stimulation by Aha1.[30]

Synergy/competition between designed compounds and a model client protein in yeast

To probe direct effects of designed activators on Hsp90 client interaction, we used the model client protein Δ131Δ.[22a] Δ131Δ was shown to stimulate ATPase[22] and its binding site was mapped to the same Hsp90 region against which the designed allosteric molecules are targeted.[22]

Yeast Hsp90 (Hsc82) ATPase activity was monitored in the presence of Δ131Δ (50 μM) or selected allosteric stimulators (**1**, **4**, **10**, **12**, **18** and **19**; 50 μM) or the combination of both (Figure 8). In contrast with the observations reported for Aha1, the benzofurans and Δ131Δ appeared to operate in a competitive fashion. Δ131Δ appeared to prevail over the compounds with relatively weaker potency (e.g., **4**, **10** and **12**), and was clearly outcompeted by the most active ligand **19**. Ligands **1** and **18** displayed a borderline behavior (Figure 8).

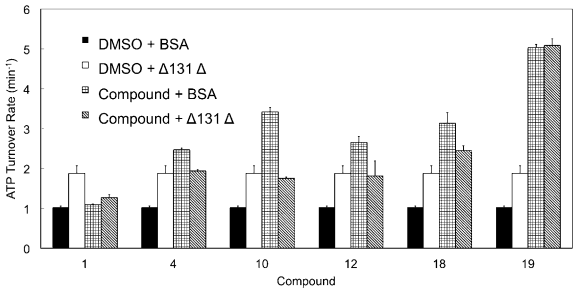

Figure 8. Competitive stimulation of yeast Hsp90 (Hsc82) ATPase by Δ131Δ and designed compounds. Hsc82 ATPase is measured in the presence of Δ131Δ (50 μM) or selected allosteric activators (50 μM, **1**, **4**, **10**, **12**, **18**, **19**) or the combination of both. Reactions with BSA and DMSO serve as negative control. Δ131Δ stimulated Hsc82 ATP-hydrolysis by 1.8-fold. The stimulation by compounds alone varies with each compound. However, when the chaperone was stimulated by both Δ131Δ and designed accelerators, the resultant ATPase rates mostly fell in the range of the rate yielded by Δ131Δ or compounds stimulation alone.

These results, combined with the analysis in the presence of Aha1, thus indicate competition between Δ131Δ and benzofuran ligands for the same binding site and for the consequent stimulation of Hsp90 ATPase.[32]

Effects of the designed compounds on cell proliferation and Hsp90 chaperone function

Given the well-established role of Hsp90 inhibition in cancer models, we asked whether our small-molecules could affect human cancer cells. The cytotoxicity of selected derivatives was examined in three human tumor cell lines of different histological origin, including breast cancer (MCF-7), castration-resistant prostate carcinoma (DU145) and diffuse malignant peritoneal mesothelioma (STO). Cells were exposed to increasing concentrations (0.1 to 100 μM) of each derivative for 72 h, and the effect on cell proliferation was determined by MTS assay (Table 2). Cytotoxic activities of glycoderivatives **4**–**16** were comparable to those of previously reported C-terminal inhibitors discovered and developed through different approaches,[33] with 50% inhibitory concentration (IC_{50}) values, as calculated from the growth curves, ranging from 29.9 to 82.3 μM.

In contrast, compounds **18** and **19**, inducing the highest ATPase stimulation in vitro, showed a remarkable and selective antiproliferative activity in the two cell models of highly chemoresistant tumors, that is, castration-resistant prostate cancer and mesothelioma, with IC_{50} values for the two compounds of 17.3 and 12.7 μM in DU145 and of 8.9 and 9.1 μM in STO, respectively (Table 2). Interestingly, compounds **18** and **19** also significantly inhibited the growth of STO-17AAG, a STO-derived cell clone with experimentally induced resistance to 17-AAG (resistance index: 32.5), as indicated by IC_{50} values comparable to those observed in the parental cell line (7.1 and 7.5 μM for compounds **18** and **19**, respectively; Table 2). Overall, these findings suggest that in these specific drug-resistant cell types

© 2015 Wiley-VCH Verlag GmbH & Co. KGaA, Weinheim

Table 2. Cytotoxic activity of **1** and derivatives **4**–**19** in three different cell lines (MCF-7, DU145, STO).[a]

	IC_{50} [μM]			
Cpd	MCF-7	DU145	STO	STO-17AAG
1	58.9 ± 7.4	63.2 ± 2.0	57.0 ± 2.1	
4	57.6 ± 3.9	66.3 ± 6.6	59.7 ± 1.5	
5	60.0 ± 4.3	61.5 ± 3.4	59.5 ± 5.1	
6	82.3 ± 6.2	64.8 ± 2.8	68.4 ± 6.2	
7	70.3 ± 9.5	68.2 ± 8.2	60.6 ± 8.4	
8	n.a.	n.a.	n.a.	
9	54.5 ± 5.7	59.4 ± 4.7	40.9 ± 3.2	
10	56.4 ± 4.6	50.7 ± 7.1	29.9 ± 1.4	
11	n.a.	n.a.	n.a.	
12	77.2 ± 0.4	60.9 ± 5.8	74.9 ± 1.8	
13	41.4 ± 4.2	55.3 ± 1.6	43.6 ± 4.5	
14	61.8 ± 5.4	58.8 ± 4.9	50.0 ± 1.3	
15	62.0 ± 6.3	63.3 ± 5.3	60.4 ± .3.0	
16	61.2 ± 2.7	52.5 ± 5.7	61.9 ± 4.7	
17	n.a.	n.a.	n.a.	
18	56.6 ± 3.9	17.3 ± 2.6	8.9 ± 1.1	7.1 ± 1.6
19	51.3 ± 4.0	12.7 ± 2.5	9.1 ± 1.1	7.5 ± 1.2
17-AAG			0.08 ± 0.01	2.6 ± 0.1

[a] Data are reported as IC_{50} values (concentration of drug required to inhibit growth by 50%) determined by MTS assay after 72 h of continuous exposure to each compound; data represent mean values ± SD of at least three independent experiments; n.a.: not assessed.

types. Compounds **10**, **12**, and **18** feature a mixed behavior dependent on the cell type. At this stage, it is particularly hard to define specific structure–activity relationships for this chemical series. Given the dynamic nature of the allosteric site and of the possible binding modes of the compounds, SARs are expectedly very complex, especially when comparing in vitro values to potency in cellular assays. On the basis of the present observations, we speculate that the L-Rha moiety (compounds **1** and **4**) may sterically perturb the assembly of the Hsp90/co-chaperone/client protein complex in the cellular context. On the other hand, the strong ATPase and conformational acceleration induced by **19** might impact the kinetic balance of the chaperone cycle, disrupting it by changing the timing and populations of Hsp90 structures that are presented to the other partners necessary to complete the folding machinery. The net result would be a degradation of the efficiency of a complex system that is normally regulated through the delicate balance of multiple factors. Deeper investigations are however needed to quantitatively support this point.

Overall, our results clearly point to a role of the designed allosteric compounds in targeting Hsp90 and its associated biological pathways, although we still have no evidence that the antiproliferative effects observed in tumor cells are exerted

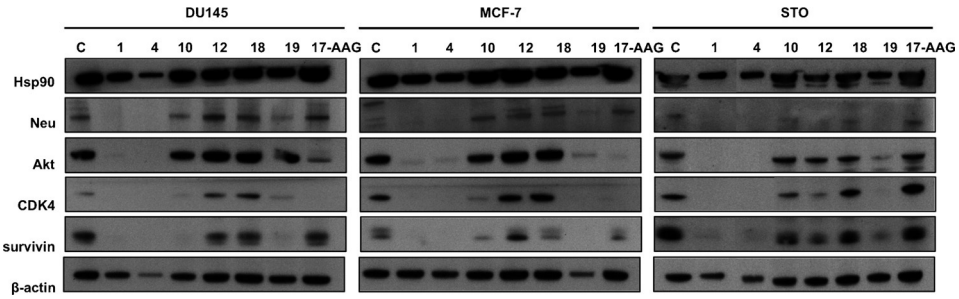

Figure 9. Inhibition of Hsp90 chaperone function. Loss of Hsp90 client proteins in human cancer cells treated for 72 h with compounds **1**, **4**, **10**, **12**, **18**, **19** or **17**-AAG (IC_{50}) and analyzed by Western blotting. β-Actin was used to confirm equal protein loading on the gel.

the Hsp90 machinery could populate an ensemble of conformations more sensitive to the new derivatives.

Moreover, the activating compounds did not disrupt the Hsp90/HSF1 complex (Figure S4 in the Supporting Information) and did not promote heat shock factor 1 (HSF1) dissociation, as classical N-terminal inhibitors are known to do.[19a] HSF1 dissociation is indeed the first step triggering the heat shock response that limits the application of NTD inhibitors in anticancer therapy. The inability of the benzofurans to activate this response is a promising feature for further development of these compounds towards therapeutic applications.

To verify whether the observed cytotoxic activity was due to the breakdown of multiple cell survival pathways as a consequence of the interaction of our compounds with Hsp90, we assessed the effects of the treatment on the stability of Hsp90 client proteins (Figure 9). Cells were exposed to selected compounds (**1**, **4**, **10**, **12**, **18** and **19**) at their IC_{50} concentration, and the amounts of Hsp90 client proteins Neu, Akt, Cdk4 and survivin were estimated in cell lysates by Western blotting (Figure 9). The client levels were significantly altered in a cell-dependent and compound-dependent fashion. In contrast, Hsp90 expression was not affected (Figure 9). Interestingly, compounds **1** and **4**, which show the lower levels of Hsp90 activation, and compound **19**, the strongest stimulator, appear to strongly decrease the levels of all clients in all examined cell solely by Hsp90 modulation. Naturally, potential off-target effects represent an important issue to investigate, albeit outside of the scopes of this study. Clearly, additional structural and mechanistic studies, along with an expanded collection of analogues, will be required to achieve quantitative SAR.

Model for Hsp90 function with allosteric ligands

The results described above suggest a complex role for Hsp90 activation. In vitro, the presence of the allosteric modulators increased yeast Hsp90 closure and ATPase rate. In cellular models, the relative effects of the activators were likely reduced due to several factors, including membrane permeation, chaperone abundance and the dynamic nature of the Hsp90 chaperone network, which favors population of different Hsp90 conformations stabilized by interactions with different multiprotein complexes.[34] In this scenario, the allosteric molecules likely bind a subset of Hsp90 molecules at any given

© 2015 Wiley-VCH Verlag GmbH & Co. KGaA, Weinheim

time, leaving the rest available for normal client and co-chaperone interactions.

To generate a structural model of the mechanism, we carried out MD simulations of the closed ATP-bound Hsp90 in complex with **1**, **4**, **10**, **12**, **18**, and **19** at the C-terminal site and compared the results with those obtained in the absence of compounds (ATP-only). MD simulations were aimed to shed light on the microscopic perturbations of Hsp90 internal dynamics induced by allosteric ligands that could be linked to the activation of functional states.

We first characterized the overall rigidity/flexibility patterns in the complexes using the coordination propensity (CP) analysis[20a] (Figure S5 in the Supporting Information). In the presence of the compound, the NTDs from one protomer were decoupled from the MD and CTD of the other. By contrast, the high degree of internal coordination between the NTD and MD within each protomer was maintained upon compound addition. In this picture, high intraprotomer coordination of the two domains favors the proper positioning of the residues necessary for catalysis, while interprotomer flexibility can be aptly exploited to speed up the search for the closed active state, consistent with the observed increases in ATPase and closure rates.

The analysis of the effects of compounds on the internal dynamics of Hsp90 highlighted interesting differences. For example, compounds **1** and **19**, representing the starting lead and the strongest activator, respectively, appear to determine different coordination patterns (Figure S4 in the Supporting Information). In particular, the coordination patterns in the different subdomains of the two protomers indicate that the dynamics of Hsp90 in the presence of **1** is more similar to the ATP-only case than in the presence of **19**. In the latter, the two protomers are moreover characterized by a highly asymmetric dynamic organization: in protomer A, in fact, high coordination entails all the NTD and M-large regions, which emerge as a coherent dynamic domain as defined by Morra et al.[20] The subdomains of protomer B, on the other hand, show the same patterns observed for the ATP-only and Hsp90-**1** cases.

Consistent with the above observations, representative structures for the complex with **19** showed an evident distortion of one of the two protomers, suggesting a role for the allosteric ligands in shifting the population to a closed asymmetric state reminiscent of the one observed in the crystal structure of the mitochondrial isoform of Hsp90 (named TRAP1).[14d] This state was also identified in solution with SAXS measurements as a general conformation of all Hsp90 chaperones, as a high-energy state that facilitates ATP hydrolysis[14d,35] (Figure 10).

Rearrangement to an asymmetric state could help explain the observed synergistic activation by Aha1, through the selection of Hsp90 conformations more favorable for co-chaperone binding, a model supported by our data in yeast lysates. Consistent with the general model of asymmetric Hsp90 activation,[14d] ligand-induced structural asymmetry in Hsp90 could determine an expansion of conformations that are primed for ATP processing and activated for Aha1 recognition. Aha1 activation was in fact shown to be asymmetric,[36] one Aha1 molecule per Hsp90 dimer is sufficient to bridge the two protomers, stabilizing the N-dimerized catalytic state. In our model, the allosteric ligands could preorganize an asymmetric Hsp90 conformation with which Aha1 preferentially interacts, stimulating ATP hydrolysis.

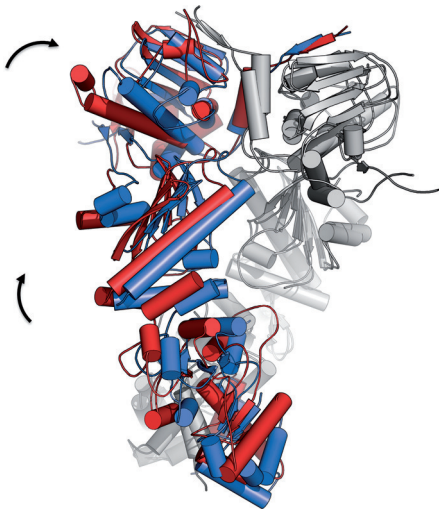

Figure 10. The structural changes induced on Hsp90 by **19** compared to the symmetric 2CG9 structure. The superposition exemplifies the distortion induced by the small molecules in protomer B (in red) compared to the original X-ray structure (PDB ID: 2CG9, in blue). Protomer A from both structures are highly superimposable and are shown in light gray for simplicity.

In the light of in vitro and cell results, we thus suggest that allosteric ligands act as conformational catalysts bringing Hsp90 into an asymmetric state primed for sequential ATP hydrolysis steps as proposed by Lavery et al.[14d] As an important caveat, it must be underlined that the data obtained from MD simulations and coordination analysis must be considered mostly qualitative: they indicate possible mechanistic differences among different protein complexes that can be linked to the observed small-molecule modulations of yeast Hsp90 ATPase. However, they do not indicate quantitative trends between dynamic variables and experimental ATPase stimulation data.

In summary, our findings indicate that the designed allosteric accelerators represent novel chemical tools to investigate salient aspects of the relationships between Hsp90 structural dynamics and functional regulation. These gain-of-function probes offer the possibility to address the role of enzymatic and conformational dynamics in the protein endogenous environment. This would complement biochemical and molecular biology approaches in shedding light on the roles of Hsp90 mechanisms at different stages of the chaperone cycle.[30,37] The observed cytotoxic activities in geldanamycin-resistant cancer cells and the lack of heat shock response induction indicate possible therapeutic perspectives for this class of compounds.

Conclusion

Proteins participate in biochemical interaction networks by switching among structural substates, which favor adaptation

© 2015 Wiley-VCH Verlag GmbH & Co. KGaA, Weinheim

to different partners and fine-tuning of functions. Such conformational changes are induced by several factors, including ligand binding.

Herein, we rationally designed new allosteric ligands of the molecular chaperone Hsp90, with the goal of exploring their biochemical and cellular effects. The initial set of molecules, **4**–**16**, was developed on the basis of compound **1**, which was previously proven to bind Hsp90-CTD and to have promising anticancer effects.[16] Interestingly, when probed in ATPase and FRET kinetic experiments, these compounds turned out to be activators of the enzymatic activity and conformational dynamics of the chaperone. Starting from this intriguing observation, we combined computational biology, synthetic chemistry, biochemical, biophysical and cell biology approaches, to design and partially optimize compounds **17**–**19** to further increase ATPase activities. These latter molecules may be considered as new molecular probes able to act as chemical switches tuning the properties of the molecular chaperone Hsp90.

The ligands were directed towards an allosteric pocket recently identified in Hsp90 by coordination propensity analysis of extended dynamic simulations of the protein. This pocket is located at the interface between the CTD and the M-domain and is dynamically coordinated to the ATP-binding site in the NTD, so that modification of the allosteric pocket are translated into variation of the ATPase activity of Hsp90. Given the intrinsically flexible nature of allosteric pockets, computational strategies for the discovery of allosteric ligands need to be developed ad hoc. Flexibility has so far hampered the resolution of crystal structures with Hsp90 complexed to C-terminal targeted ligands. Here we turned to extensive molecular dynamics simulation of the protein in the presence of a lead compound (**1**), previously identified by virtual screening in a pharmacophore model and validated as a CTD binder and an allosteric modulator by a number of experimental techniques.[16] The identification of the ligand–protein interactions most relevant in determining the dynamic cross-talk between the binding partners guided the evolution of initial activators towards molecules with higher activities. Computational results pointed to specific charged and hydrophobic residues in the putative Hsp90 allosteric pocket that could be targeted by ligands designed to contain specific and complementary chemical functionalities.

In particular, these results showed that the sugar moiety of **1** interacts extensively with the protein and suggested to expand the SAR by glycodiversification of the aglycon of **1** (**2**) and of its synthetic precursor **3**. Analysis of the interaction of compounds **4**–**16** with Hsp90 revealed that most of them act as stimulators, rather than inhibitors, of the ATPase activity, a feature that was totally unprecedented, until very recently[27] activators were found by large scale screening. We would like to underline that the case we present here is the first one where these results are obtained using *a rational design approach*. The validity of our protocol was further corroborated by the development of second generation activators: additional modeling reinforced the starting pharmacophoric hypothesis and suggested a second set of modifications, finally leading to **19**, which accelerates Hsp90 ATPase by a factor of six, similar to the most active known endogenous activator, the co-chaperone Aha1.

Using FRET, we showed that ATPase activation by the benzofuran probes is connected to acceleration of Hsp90 conformational dynamics. We characterized the activity of the most potent probes in the presence of the endogenous activator Aha1, which is known to bind the N-M domains of Hsp90 and thus in principle should not compete with the ligands, and of the model client protein $\Delta131\Delta$, which binds in the proximity of the proposed allosteric site. Importantly, the allosteric ligands showed a synergistic effect with Aha1 and a competition with $\Delta131\Delta$ in regulating Hsp90 ATPase. Consistent with the synergistic effect with Aha1, co-immunoprecipitation experiments also showed that association of the Hsp90 ATPase inhibitory co-chaperone Sba1 was reduced in the presence of benzofuran stimulators. Finally, the stimulatory activity observed on the isolated protein was found to translate to cytotoxicity in specific cell lines, which are known to be sensitive to Hsp90 deregulation. The molecules tested were shown to affect the viability of cancer cells, in particular those resistant to the Hsp90-targeted drug 17AAG, providing new opportunities to generate anticancer interventions based on novel mechanisms of action. Remarkably, the benzofurans described here were shown not to activate the heat shock response in treated cells, a known drawback of Hsp90 NTD inhibitors.

Whether activation of the chaperone is the only mechanism operating in cellular studies, it still needs to be fully demonstrated. Nonetheless, these designed allosteric activators may represent innovative gain-of-function probes to directly address the roles of Hsp90 ATPase and conformational dynamics in determining its cell functions. Moreover, our approach may ultimately generate effective anticancer drugs with novel mechanisms of action, based on the perturbation of the Hsp90 machinery, whereby the acceleration of conformational dynamics can eventually translate into impaired chaperone functions and cell death.

Experimental Section

Design and synthesis

Docking calculations and MD simulations: Docking was carried out with the Maestro Suite (Release 2013-1-9.4, Schrödinger, LLC, New York, NY, 2013). The shape and chemical properties of the CTD binding site were mapped onto a grid with dimensions of 36 Å (enclosing box) and 14 Å (ligand diameter midpoint box). Docking calculations were performed using Glide[38] (version 5.8) and carried out in XP-mode with the OPLS-AA force field.[39] The resulting consensus poses were used for molecular dynamics simulation.

The structures of the three most populated clusters for complexes with **1**, **4**, **10**, **12**, **18**, **19** were used to start 100 ns explicit solvent MD. Three simulations were run for each complex (total of 1800 ns). Control simulations were run with Hsp90 in complex with ATP only. All calculations were carried out with GROMACS.[40] Details are provided in the Supporting Information.

Synthesis of allosteric ligands: Synthesis of compounds **1**–**16** was described previously.[25] For **17**–**19**, aglycon **3** was treated with dif-

© 2015 Wiley-VCH Verlag GmbH & Co. KGaA, Weinheim

ferent alkylating agents under phase-transfer catalysis conditions analogous to those previously reported.[25] Details of the synthesis and full compound characterization are collected the in Supporting Information.

Biochemical and biophysical assays

Hsp90 ATPase assay: ATPase activity of Hsp90 was measured by the NADH-coupled ATPase assay. Briefly, Hsc82 (2 μM) or human Hsp90α (2 μM) was premixed with NADH (0.18 μM), L-lactate dehydrogenase (50 U mL^{-1}), PEP (1 mM), pyruvate kinase (50 U mL^{-1}) and compounds (dissolved in DMSO to a final concentration of 50 μM; 5 μM for radicicol). The reaction was initiated by the addition of ATP (1 mM). The reaction was carried out at 30 °C in buffer composed of HEPES (20 mM, pH 7.5), KCl (100 mM) and $MgCl_2$ (1 mM). Absorbance data were collected using a microplate spectrophotometer (Spectra M5, Molecular Devices) at 360 nm.

FRET-based Hsp90 conformational change assay: The conformational change rate of Hsp90 was measured by a FRET-based assay.[41] Briefly, D61C or E329C mutation was introduced into Hsc82 for labeling with Alex Fluor 647 or Alex Fluor 555 (Life Technologies), respectively. Labeled Hsp90 populations were mixed to produce Hsp90 heterodimers. The conformational change of Hsp90 was initiated by adding AMP-PNP (1 mM) in the presence of compounds. The fluorescence from different dyes was monitored on a microplate spectrophotometer with excitation/emission wavelength as follows: Ex525/Em568 (AF555), Ex525/Em668 (AF647). The assay was carried out at room temperature in the same buffer as Hsp90 ATPase assay.

Cytotoxicity and effects on Hsp90 interactions of designed compounds

Cell lines: Human breast cancer (MCF-7) and castration-resistant prostate carcinoma (DU145) cell lines were obtained from the American Type Culture Collection (Rockville, MD, USA). The human diffuse malignant peritoneal mesothelioma cell line (STO) was established from a tumor specimen of a patient who underwent surgery at the Istituto Nazionale dei Tumori, Milan.[42] The resistant subline STO-17AAG was derived by continuous exposure of the original parental cell line (STO) to increasing concentrations of 17-AAG.

Cell proliferation assay: After harvesting in the logarithmic growth phase, 4500 cells per 50 μL were plated in 96-well flat-bottomed microtiter plates for 24 h and treated with increasing concentrations of CTD ligands (1–100 μM) or 17-AAG (0.05–50 μM) for 72 h. Control cells received vehicle alone (DMSO). At the end of drug exposure, cell growth inhibition was determined with the CellTiter 96® AQueous one solution cell proliferation assay (MTS; Promega). Optical density was read at 490 nm on a microplate reader (POLARstar OPTIMA) and the results were expressed as a percentage relative to DMSO-treated cells. Dose-response curves were created and IC_{50} values were determined graphically from the curve for each compound.

Analysis of Hsp90 client proteins: To monitor changes in Hsp90 client proteins, cells were harvested, solubilized in lysis buffer (0.01% NP40, 10 mM Tris pH 7.5, 50 mM KCl, 5 mM $MgCl_2$, 2 mM DTT, 20% glycerol plus protease inhibitors) and analyzed by Western blotting primary antibodies specific for survivin (AbCam), Hsp90, CDK4, Neu (Santa Cruz Biotechnology), and Akt (Cell Signaling Technology). Briefly, total cellular lysates were separated on a 4–12% NuPAGE bis-tris gel (Life Technologies) and transferred to nitrocellulose using standard protocols. The filters were blocked in PBS 1×Tween-20 with 5% skim milk or 5% BSA and incubated, overnight, with primary antibodies. The filters were then incubated with the secondary peroxidase-linked whole antibodies (Life Technologies). Bound antibodies were detected using the Novex ECL, HRP chemiluminescent substrate reagent kit (Life Technologies). Filters were autoradiographed and images were acquired by Biospectrum imaging system (Ultra-Violet Products Ltd.). β-Actin (AbCam) was used on each blot to ensure equal loading of proteins.

Hsp90 co-chaperone interaction analysis (Co-IP analysis): Yeast expressing His-tagged Hsc82 (yeast Hsp90) as their sole Hsp90 protein (yeast strain pp30 [hsc82hsp82]) were lysed as previously described.[43] Protein lysates were incubated either with buffer (− negative control) or with 5 mM AMP-PNP as indicated, as well as with 50 μM allosteric compounds, for 10 min at 30° prior to affinity precipitation of His-tagged Hsp82 with Ni-NTA agarose. Hsp82-associated Sba1 was detected by immunoblotting.

Acknowledgements

We acknowledge funding from Fondazione Cariplo through grant 2011.1800, "Premio Fondazione Cariplo per la Ricerca di Frontiera". G.C. acknowledges funding from the AIRC (Associazione Italiana Ricerca sul Cancro) grant IG 15420; Universita' degli Studi di Milano is acknowledged for a grant to S.S. (Assegno di ricerca tipo A).

Keywords: allostery · drug design · functional dynamics · glycoconjugates · Hsp90

[1] R. Nussinov, C.-J. Tsai, *Cell* **2013**, *153*, 293 – 305.
[2] a) V. J. Hilser, *Science* **2010**, *327*, 653 – 654; b) R. G. Smock, L. M. Gierasch, *Science* **2009**, *324*, 198 – 203.
[3] J. A. Zorn, J. A. Wells, *Nat. Chem. Biol.* **2010**, *6*, 179 – 188.
[4] a) Z. Fang, C. Grütter, D. Rauh, *ACS Chem. Biol.* **2013**, *8*, 58 – 70; b) C. J. Wenthur, P. R. Gentry, T. P. Mathews, C. W. Lindsley, *Rev. Pharm. Toxicol.* **2014**, *54*, 165 – 184; c) A. Rodina, P. D. Patel, Y. Kang, Y. Patel, I. Baaklini, M. J. Wong, T. Taldone, P. Yan, C. Yang, R. Maharaj, A. Gozman, M. R. Patel, H. J. Patel, W. Chirico, H. Erdjument-Bromage, T. T. Talele, J. C. Young, G. Chiosis, *Chem. Biol.* **2013**, *20*, 1469 – 1480.
[5] M. Taipale, D. F. Jarosz, S. Lindquist, *Nat. Rev. Mol. Cell. Biol.* **2010**, *11*, 515 – 528.
[6] S. E. Jackson, *Top. Curr. Chem.* **2013**, *328*, 155 – 240.
[7] L. Whitesell, S. Lindquist, *Nat. Rev. Cancer* **2005**, *5*, 761 – 772.
[8] V. Shah, R. Wiest, G. Garcia-Cardena, G. Cadelina, R. J. Groszmann, W. C. Sessa, *Am. J. Physiol.* **1999**, *277*, 463 – 468.
[9] W. Luo, W. Sun, T. Taldone, A. Rodina, G. Chiosis, *Mol. Neurodegener.* **2010**, *5*, 24.
[10] D. F. Jarosz, S. Lindquist, *Science* **2010**, *330*, 1820 – 1824.
[11] M. Taipale, I. Krykbaeva, M. Koeva, C. Kayatekin, K. D. Westover, G. I. Karras, S. Lindquist, *Cell* **2012**, *150*, 987 – 1001.
[12] a) P. C. Echeverría, A. Bernthaler, P. Dupuis, B. Mayer, D. Picard, *PLoS ONE* **2011**, *6*, e26044; b) E. Kirschke, D. Goswami, D. Southworth, P. R. Griffin, D. A. Agard, *Cell* **2014**, *157*, 1685 – 1697.
[13] K. A. Krukenberg, T. O. Street, L. A. Lavery, D. A. Agard, *Q. Rev. Biophys.* **2011**, *44*, 229 – 255.
[14] a) M. M. U. Ali, S. M. Roe, C. K. Vaughan, P. Meyer, B. Panaretou, P. W. Piper, C. Prodromou, L. H. Pearl, *Nature* **2006**, *440*, 1013 – 1017; b) A. K. Shiau, S. F. Harris, D. R. Southworth, D. A. Agard, *Cell* **2006**, *127*, 329 – 340; c) D. E. Dollins, J. J. Warren, R. M. Immormino, D. T. Gewirth, *Mol. Cell* **2007**, *28*, 41 – 56; d) L. A. Lavery, J. R. Partridge, T. A. Ramelot, D. Elnatan, M. A. Kennedy, D. A. Agard, *Mol. Cell* **2014**, *53*, 330 – 343.
[15] a) A. Zuehlke, J. L. Johnson, *BIOPOLYMERS* **2010**, *93*, 211 – 217; b) J. Li, J. Buchner, *Biomed. J.* **2013**, *36*, 106 – 117.

© 2015 Wiley-VCH Verlag GmbH & Co. KGaA, Weinheim

[16] G. Morra, M. A. C. Neves, C. J. Plescia, S. Tsutsumi, L. Neckers, G. Verkhivker, D. C. Altieri, G. Colombo, *J. Chem. Theory Comput.* **2010**, *6*, 2978 – 2989.
[17] M. Taddei, S. Ferrini, L. Giannotti, M. Corsi, F. Manetti, G. Giannini, L. Vesci, F. M. Milazzo, D. Alloatti, M. B. Guglielmi, M. Castorina, M. Cervoni, M. Barbarino, R. Foderà, V. Carollo, C. Pisano, S. Armaroli, W. Cabri, *J. Med. Chem.* **2014**, *57*, 2258 – 2274.
[18] S. M. Roe, C. Prodromou, R. O'Brien, J. E. Ladbury, P. W. Piper, L. H. Pearl, *J. Med. Chem.* **1999**, *42*, 260 – 266.
[19] a) P. Workman, F. J. Burrows, L. Neckers, N. Rosen, *Ann. N. Y. Acad. Sci.* **2007**, *1113*, 202 – 216; b) L. Whitesell, R. Bagatell, R. Falsey, *Curr. Cancer Drug Targets* **2003**, *3*, 349 – 358.
[20] a) G. Morra, R. Potestio, C. Micheletti, G. Colombo, *PLoS Comput. Biol.* **2012**, *8*, e1002433; b) G. Morra, G. M. Verkhivker, G. Colombo, *PLoS Comput. Biol.* **2009**, *5*, e1000323.
[21] a) E. Moroni, H. Zhao, B. S. Blagg, G. Colombo, *J. Chem. Inf. Model* **2014**, 24397468; b) H. Zhao, E. Moroni, G. Colombo, B. S. Blagg, *ACS Med. Chem. Lett* **2014**, *5*, 84 – 88; c) H. Zhao, E. Moroni, B. Yan, G. Colombo, B. S. J. Blagg, *ACS Med. Chem. Lett.* **2013**, *4*, 57 – 62.
[22] a) T. O. Street, L. A. Lavery, D. A. Agard, *Mol. Cell* **2011**, *42*, 96 – 105; b) O. Genest, M. Reidy, T. O. Street, J. R. Hoskins, J. L. Camberg, D. A. Agard, D. C. Masison, S. Wickner, *Mol. Cell* **2013**, *49*, 464 – 473.
[23] E. Moroni, A. Paladino, G. Colombo, *Curr. Top. Med. Chem.* **2015**, *15*, 2043 – 2055.
[24] R. D. Goff, J. S. Thorson, *Med. Chem. Commun.* **2014**, *5*, 1036 – 1047.
[25] L. Morelli, A. Bernardi, S. Sattin, *Carbohydr. Res.* **2014**, *390C*, 33 – 41.
[26] B. Panaretou, C. Prodromou, S. M. Roe, R. O'Brien, J. E. Ladbury, P. W. Piper, L. H. Pearl, *EMBO J.* **1998**, *17*, 4829 – 4836.
[27] B. K. Zierer, M. Weiwad, M. Rubbelke, L. Freiburger, G. Fischer, O. R. Lorenz, M. Sattler, K. Richter, J. Buchner, *Angew. Chem. Int. Ed.* **2014**, *53*, 12257 – 12262; *Angew. Chem.* **2014**, *126*, 12454 – 12459.
[28] A. Kranjc, S. Bongarzone, G. Rossetti, X. Biarnes, A. Cavalli, M. L. Bolognesi, M. Roberti, G. Legname, P. Carloni, *J. Chem. Theory Comput.* **2009**, *5*, 2565 – 2573.
[29] a) M. Mickler, M. Hessling, C. Ratzke, J. Buchner, T. Hugel, *Nat. Struct. Mol. Biol.* **2009**, *16*, 281 – 286; b) D. R. Southworth, D. A. Agard, *Mol. Cell* **2008**, *32*, 631 – 640.
[30] L. Pullen, D. N. Bolon, *J. Biol. Chem.* **2011**, *286*, 11091 – 11098.
[31] J. Li, K. Richter, J. Reinstein, J. Buchner, *Nat. Struct. Mol. Biol.* **2013**, *20*, 326 – 331.
[32] S. H. McLaughlin, H. W. Smith, S. E. Jackson, *J. Mol. Biol.* **2002**, *315*, 787 – 798.
[33] H. P. Zhao, A. C. Donnelly, B. R. Kusuma, G. E. L. Brandt, D. Brown, R. A. Rajewski, G. Vielhauer, J. Holzbeierlein, M. S. Cohen, B. S. J. Blagg, *J. Med. Chem.* **2011**, *54*, 3839 – 3853.
[34] I. Fierro-Monti, P. Echeverria, J. Racle, C. Hernandez, D. Picard, M. Quadroni, *PLoS ONE* **2013**, *8*, e80425.
[35] J. R. Partridge, L. A. Lavery, D. Elnatan, N. Naber, R. Cooke, D. A. Agard, *eLife* **2014**, DOI: 10.7554/eLife.03487.
[36] M. Retzlaff, F. Hagn, L. Mitschke, M. Hessling, F. Gugel, H. Kessler, K. Richter, J. Buchner, *Mol. Cell* **2010**, *37*, 344 – 354.
[37] K. Beebe, M. Mollapour, B. Scroggins, C. Prodromou, W. Xu, M. Tokita, T. Taldone, L. Pullen, B. K. Zierer, M. J. Lee, J. Trepel, J. Buchner, D. N. Bolon, G. Chiosis, L. Neckers, *Oncotarget* **2013**, *4*, 1065 – 1074.
[38] R. A. Friesner, R. B. Murphy, M. P. Repasky, L. L. Frye, J. R. Greenwood, T. A. Halgren, P. C. Sanschagrin, D. T. Mainz, *J. Med. Chem.* **2006**, *49*, 6177 – 6196.
[39] W. L. Jorgensen, D. S. Maxwell, J. Tirado-Rives, *J. Am. Chem. Soc.* **1996**, *118*, 11225 – 11236.
[40] B. Hess, C. Kutzner, D. van der Spoel, E. Lindahl, *J. Chem. Theory Comput.* **2008**, *4*, 435 – 447.
[41] M. Hessling, K. Richter, J. Buchner, *Nat. Struct. Mol. Biol.* **2009**, *16*, 287 – 293.
[42] N. Zaffaroni, A. Costa, M. Pennati, C. De Marco, E. Affini, M. Madeo, R. Erdas, A. Cabras, S. Kusamura, D. Baratti, M. Deraco, M. G. Daidone, *Cell Oncol.* **2007**, *29*, 453 – 466.
[43] M. Mollapour, D. Bourboulia, K. Beebe, M. R. Woodford, S. Polier, A. Hoang, R. Chelluri, Y. Li, A. Guo, M. J. Lee, E. Fotooh-abadi, S. Khan, T. Prince, N. Miyajima, S. Yoshida, S. Tusutsumi, W. P. Xu, B. Panaretou, W. G. Stetler-Stevenson, G. Bratslavsky, J. B. Trepel, C. Prodromou, L. Neckers, *Mol. Cell* **2014**, *53*, 317 – 329.

Received: May 7, 2015
Published online on August 18, 2015

© 2015 Wiley-VCH Verlag GmbH & Co. KGaA, Weinheim